A Triple Mutant of the *Drosophila* ERR Confers Ligand-Induced Suppression of Activity†

Tove Östberg,‡ Micael Jacobsson,§,# Anneli Attersand,|| Alexander Mata de Urquiza,⊥ and Lena Jendeberg*,||

Department of Cell and Molecular Biology, Medical Nobel Institute, Karolinska Institute, S-171 77 Stockholm, Sweden, Departments of Structural Chemistry and Biology, Biovitrum AB, Lindhagensgatan 133, S-112 76 Stockholm, Sweden, Ludwig Institute of Cancer Research, Stockholm Branch, S-171 77 Stockholm, Sweden, and Department of Medicinal Chemistry, Uppsala University, S-751 23 Uppsala, Sweden

Received December 2, 2002; Revised Manuscript Received March 5, 2003

ABSTRACT: The steroid hormone (NR3) subfamily of nuclear receptors was until recently believed to be restricted to deuterostomes. However, a novel nuclear receptor belonging to the NR3 subfamily was recently identified in the *Drosophila melanogaster* genome, indicating the existence of an ancestor before the evolutionary split of deuterostomes and protostomes. This receptor, termed the *Drosophila* estrogen-related receptor (dERR), most closely resembles the human and mouse estrogen-related receptors (ERRs) in both the DNA binding domain (DBD) (approximately 85% identical) and the ligand binding domain (LBD) (approximately 35% identical). Here we describe the functional analysis and rational design of ligand responsive dERR mutants created by protein engineering of the LBD. On the basis of homology modeling, three amino acid residues in the LBD were identified and mutated to enable ligand-dependent suppression of transcriptional activity. Our results show that the Y295A/T333I/Y365L triple mutant is significantly suppressed by the known ERR inverse agonists 4-hydroxytamoxifen (OHT) and diethylstilbestrol (DES), in comparison to the wild-type dERR receptor, which was inefficiently suppressed by these substances. The coactivator mGRIP-1 (mouse glucocorticoid receptor interacting protein 1) was shown to significantly increase the activity of the triple mutant in transfection experiments, and the addition of OHT resulted in an efficient suppression of the activity. Accordingly, the ability to functionally interact with a coactivator is still maintained by the Y295A/T333I/Y365L mutant. These findings demonstrate the potential of using rational design and engineering of the LBD to study the function of a nuclear receptor lacking identified ligands.

One of the largest groups of transcription factors is the nuclear receptor (NR)[1] superfamily. Most NRs function as ligand inducible transcription factors that, upon interaction with their cognate ligands, regulate the expression of target genes by binding to DNA response elements (RE) in the relevant promoter regions. For a large number of receptors, no ligands have so far been identified, and these are therefore termed orphan receptors.

The first members of the orphan receptors, the estrogen-related receptors α and *β* (ERRα and ERR*β*, respectively), were identified on the basis of their amino acid homology with estrogen receptor α (ERα) (*1*), and classified as members of the NR3 subfamily (*2*). An isoform of ERRα, ERRα-1, also exists (*3*). A third member of the ERR subfamily, ERR*γ*, was more recently identified (*4*−*6*). The ERRs are considered to be constitutively active, where ERRα has the lowest and ERR*γ* the highest activity (*7*, *8*). Although the ERRs are highly homologous with the ERs, they do not bind any of the classical steroid hormones (*1*). The synthetic estrogen, diethylstilbestrol (DES), as well as the selective estrogen receptor modulator (SERM) tamoxifen (TAM) and its metabolite 4-hydroxytamoxifen (OHT) are known to suppress the activity of ERR*β* and ERR*γ* (*9*, *10*). The activity of ERRα-1 has been shown to be suppressed by two organochlorine pesticides, toxaphene and chlordane (*11*), which in contrast are weak activators of ERα (*12*). The ERRs bind DNA to repeated estrogen response elements (EREs) and to single-repeat ERR response elements (ERREs), also denoted SF-1 response elements (SFREs) (*3*, *13*−*16*).

The NR3 subfamily of the nuclear receptors was until recently believed to be restricted to deuterostomes (*17*). However, a novel NR belonging to the NR3 subfamily was

† T.Ö. was supported by a predoctoral fellowship from Biovitrum to the Karolinska Institute.

* To whom correspondence should be addressed. E-mail: lena.jendeberg@biovitrum.com. Fax: +46 86185882. Telephone: +46 86973269.

‡ Karolinska Institute.

§ Department of Structural Chemistry, Biovitrum AB.

Department of Medicinal Chemistry, Uppsala University, S-751 23 Uppsala, Sweden.

|| Department of Biology, Biovitrum AB.

⊥ Ludwig Institute of Cancer Research.

[1] Abbreviations: DBD, DNA binding domain; DES, diethylstilbestrol; EMSA, electrophoretic mobility shift assay; ER, estrogen receptor; ERE, estrogen response element; ERR, estrogen-related receptor/estrogen receptor-related receptor; ERRE, ERR response element; GRIP-1, glucocorticoid receptor interacting protein 1; HMM, hidden Markov model; ICM, internal coordinate mechanics; LBD, ligand binding domain; NR, nuclear receptor; NR3, nuclear receptor subfamily 3; OHT, 4-hydroxytamoxifen; SFRE, SF-1 response element; TAM, tamoxifen.

10.1021/bi027279b CCC: $25.00 © 2003 American Chemical Society
Published on Web 05/09/2003

recently identified in the genome of *Drosophila melanogaster* (*18*, *19*). DmCG7404 (flybase accession number) (GenBank entry AF359420), termed the *Drosophila* estrogen-related receptor (dERR), most closely resembles the ERRs in both the DNA binding domain (DBD) and the ligand binding domain (LBD) (*20*), being approximately 85 and 35% identical, respectively. Including this novel receptor, the total number of NRs in *D. melanogaster* is 21. No members of the NR3 subfamily have been found in the *Caenorhabditis elegans* genome, raising the question of whether members of the NR3 subfamily are present in other nematodes. The presence of a member of the steroid hormone receptor family in the *D. melanogaster* genome indicates also that the NR3 family (like the other five subfamilies) arose before the evolutionary split of protostomes and deuterostomes, as discussed previously by Maglich et al. (*20*).

Little is known about the mechanism of activation of invertebrate NRs. A number of the *D. melanogaster* NRs are highly divergent from the other superfamily members in their complete lack of the LBD. These receptors are thought to function in a ligand-independent manner (*21*). Ecdysone is a steroid known to have biological activity in *D. melanogaster*. This steroid is a ligand for the ecdysone receptor, and it also regulates approximately half of the known *D. melanogaster* NRs indirectly (*21*).

Here we present studies of the dERR, the recently identified *D. melanogaster* member of the NR3 subfamily. We have cloned and verified the predicted dERR sequence, and studies *in vitro* indicate functional DNA binding of the dERR to ERRE and ERE, resulting in transcriptional activation. Since the transcriptional activity of the dERR was inefficiently suppressed by the known ERR inverse agonists, we decided to test if ligand-induced suppression could be achieved by a limited number of site specific mutations. On the basis of homology modeling of the dERR LBD, using the structure of hERα bound to 4-hydroxytamoxifen [PDB entry 3ert (*22*)] as a template, three amino acid residues potentially implicated in ligand interaction were identified and subsequently mutated. With functional studies, we show that the predicted amino acid substitutions confer ligand-induced suppression of dERR activity.

MATERIALS AND METHODS

Cloning of the dERR. The prerelease of the *D. melanogaster* genome (shotgun fragments prior to the genome assembly) from Celera was used to search for and investigate previously unknown members of the nuclear receptor superfamily. Multiple alignments of the DBD of selected receptors were constructed manually (*23*) to create a hidden Markov model (HMM) of the DBD. The HMMs were built using HMMER version 1.8.3 (*24*), and the model was used to search the complete genome. The 5′ and 3′ ends of the identified nuclear receptor, termed the dERR, were cloned by RACE-PCR as previously described (*25*). The full-length receptor was cloned with gene specific primers: full-length dERR (5′), 5′-TACGGATCCATGGCCGACGGCGTCAGC; full-length dERR (3′), 5′-AAGGAAAAAAGCGGCCGCTCACCTGGCCAGCGGCTC.

DNA Constructs for Full-Length Receptor Analysis. The dERR receptor was subcloned into the pCDNA3 vector (Invitrogen). Full-length mERRβ was generated by PCR amplification from a previously described plasmid (*15*), and the following primers were used: full-length mERR (5′), 5′-GGTACCACCATGTCGTCCGAAGACAGGCAC; full-length mERR (3′), 5′-CTCGAGTCACACCTTGGCCTCCAGCAT. The mERRβ receptor was subcloned into the pCDNA3 vector (Invitrogen). PFU polymerase (Stratagene) was used for PCR amplification. For the response element constructs, complementary linkers containing 3× ERRE or 3× ERE (recognition sequences are underlined) were annealed and inserted upstream of the simian virus 40 promoter in the pGL2-promoter plasmid (Promega): ERRE (5′) linker, 5′-CCGGACCTCAAGGTCACGTTCGGACCTCAAGGTCACGTTCGGACCTCAAGGTCAGGATCCA; ERRE (3′) linker, 5′-GATCTGGATCCTGACCTTGAGGTCCGAACGTGACCTTGAGGTCCGAACGTGACCTTGAGGTCCGGGTAC; ERE (5′) linker, 5′-CCGGACCAGAGGTCACTGTGACCTCTCGTTCGGACCAGAGGTCACTGTGACCTCTCGTTCGGACCAGAGGTCACTGTGACCTCTGGATCCA; ERE (3′) linker, 5′-GATCTGGATCCAGAGGTCACAGTGACCTCTGGTCCGAACGAGAGGTCACAGTGACCTCTGGTCCGAACGAGAGGTCACAGTGACCTCTGTCCGGGTAC. All constructs were confirmed by sequence analysis.

DNA Constructs for GAL4−LBD Fusion Analysis. The ligand binding domains of the dERR and mERRβ receptors were generated by PCR amplification using PFU polymerase (Stratagene) and subcloned into the pCMXGal4 vector, containing the GAL4−DBD (*26*). The following primers were used: dERR-LBD (5′), 5′-TATGGTACCACTAATGATGAGGCCTCATCC; dERR-LBD (3′), 5′-TATGGATCCTCACCTGGCCAGCGGCTC; mERR-LBD (5′), 5′-GGTACCATGCTGAAGGAAGGTGTGCGC; mERR-LBD (3′), 5′-CCTAGGTCACACCTTGGCCTCCAGCAT. Mutations at three different amino acids were introduced: Y295A, T333I, and Y365L. A triple mutant (Y295A/T333I/Y365L), a double mutant (T333I/Y365L), and a single mutant (Y295A) were designed. The mutations were introduced by PCR mutagenesis in a two-step reaction. The following primers were used (mutations are shown in lowercase letters): LBD (5′), 5′-TATGGTACCACTAATGATGAGGCCTCATCC; LBD (3′), 5′-TATGGATCCTCACCTGGCCAGCGGCTC; Y295A (5′), 5′-TTAGTGATATcgcaGACAAGGAAT; Y295A (3′), 5′-ATTCCTTGTCtgcgATATCACTAA; T333I (5′), 5′-AGAGATCCTGatcCTCCAGCTGA; T333I (3′), 5′-TCAGCTGGAGgatCAGGATCTCT; Y365L (5′), 5′-GGAGTGCGTttaACGGAATTCT; Y365L (3′), 5′-AGAATTCCGTtaAACCGCACTCC. The mutant LBDs were subcloned into the pCMXGal4 vector. All constructs were verified by DNA sequencing. The 4xGAL4-RE luciferase reporter plasmid has been described previously (*26*).

General Plasmids. The pRSV-AF control plasmid for transfection normalization was previously described (*27*). The mGRIP-1 plasmid used for expression of full-length mouse GRIP-1 (also denoted TIF-2) was a kind gift from E. Treuter (CBT, Karolinska Institute).

Electrophoretic Mobility Shift Assay (EMSA). The dERR and mERR proteins were translated *in vitro* using the TNT Quick coupled transcription/translation system (Promega) according to the manufacturer's recommendations. Complementary oligonucleotides, containing either the ERRE or ERE sequences, were annealed and labeled with [^{32}P]-

dCTP by Klenow polymerase (New England Biolabs) fill-in reactions, according to the manufacturer's recommendations. Binding reactions were performed in a buffer containing 10 mM Tris-HCl (pH 8.0), 40 mM KCl, 0.1% NP-40, 60% glycerol, and 1 mM DTT, supplemented with protease inhibitors and 0.2 μM poly(dI-dC). One microliter of the respective probe and 4 μL of translation product were mixed with binding buffer to a final volume of 20 μL. A 100-fold molar excess of unlabeled oligonucleotides was used for competition in the indicated lanes. The reaction products were analyzed by 4% polyacrylamide gel electrophoresis, and the results were visualized using a phosphorimager (Molecular Dynamics). The following oligonucleotides were used (recognition sites are underlined and mutations are in lowercase letters): ERRE (5′), 5′-AGCAGTGGCGATTGTCAAGGTCA; ERRE (3′), 5′-ACTGTGTGACCTTGACAATCGCCA; ERREmut (5′), 5′-AGCAGTGGCGATTGTCAAGtaCA; ERREmut (3′), 5′-ACTGTGTGtaCTTGACAATCGCCA; ERE (5′), 5′-ACGGGTAGAGGTCACTGTGACCTCTA; ERE (3′), 5′-CGGGTAGAGGTCACAGTGACCTCTA; EREmut (5′), 5′-ACGGGTAGAGtaCACTGTGtaCTCTA; EREmut (3′), 5′-CGGGTAGAGtaCACAGTGtaCTCTA.

Reporter Gene Assays. (1) Full-Length Receptors. All transient transfection experiments were performed in CaCo-2 subclone TC7 (CaCo-2/TC7) cells in six-well plates. Cells were seeded at a concentration of 2×10^5 cells per well and incubated for 24 h at 37 °C in 2 mL of growth medium containing Dulbecco's modified Eagle's medium (DMEM), 10% fetal bovine serum (FBS), nonessential amino acids (NEA) (10 mL/L), and glutamine (GLUT) (20 mL/L). (DMEM was purchased from SVA. FBS, NEA, and GLUT were purchased from Life Technologies.) The medium was replaced with 2 mL of transfection medium containing Optimem (Invitrogen) and 10% charcoal/dextran-treated fetal bovine serum (Hyclone). The cells were cotransfected with 0.075 μg of receptor plasmid, 3 μg of reporter plasmid, and 0.1 μg of RSV-AF plasmid (alkaline phosphatase activity was used for normalization of transfection efficiency) using FuGENE-6 (Roche) according to the manufacturer's instructions. Where indicated, 0.075 μg of coactivator plasmid (mGRIP-1) was cotransfected. After 20−24 h, the medium was replaced (Optimem, 2% charcoal/dextran-treated fetal bovine serum). Following incubation for 24 h, the medium was analyzed for alkaline phosphatase activity according to the manufacturer's recommendations (Great EscAPe SEAP, Promega). Cells were harvested in lysis buffer (0.1 M Tris, 2 mM EDTA, and 0.25% Triton X-100), and the cell lysates were analyzed for luciferase activity with a Luciferase assay kit (BioThema AB). All experiments were performed at least three times in duplicate, and luciferase activity was normalized for alkaline phosphatase activity and subsequently divided by reporter activity of pCDNA3 lacking an insert.

(2) GAL4−LBD Fusions. GAL4−LBD transfections were performed as described above with the following exception: the cells were cotransfected with 2 μg of 4xGAL4-RE luciferase reporter and 0.2 μg of dERRwt/mERRwt/dERR mutant plasmid (where the LBD of the receptor is fused to the GAL4−DBD). Where indicated, 0.2 μg of coactivator plasmid (mGRIP-1) was cotransfected. After 24 h, cells were treated with tamoxifen (TAM), 4-hydroxytamoxifen (OHT), or diethylstilbestrol (DES), dissolved in DMSO. As a control, cells were treated with the same amount of DMSO (0.1%). The chemicals were purchased from Sigma.

Protein Modeling of the dERR Ligand Binding Domain. Homology modeling was performed by molecular mechanics energy minimization of the model structure with restraints derived from the template structure, using the internal coordinate mechanism (ICM) software (*28*). All aligned residues in the model were tethered to the corresponding residues in the template structure, using harmonic restraints centered on the template residues. Tethers were not set for one flanking residue on each side of an insertion gap or three flanking residues of a deletion gap. The minimization procedure was carried out in a simulated annealing-type four-step procedure. A starting model was built by minimizing the harmonic restraints only. The side chain conformations were sampled using Biased Probability Monte Carlo (*28*) minimization. Both side chain and backbone conformations of all loops (marked by magenta in Figure 5) and flanking residues were sampled, and finally, the side chain conformations were sampled again, using a more sensitive but less robust force field for the energy calculations.

RESULTS

Cloning of dERR. Using hidden Markow models (HMMs), a novel nuclear receptor termed dERR, belonging to the NR3 family, was identified. dERR was cloned and verified by sequence analysis, resulting in a DNA fragment encoding a protein of 482 amino acid residues. The deduced amino acid sequence was homologous to those of the human and mouse ERRs [also shown by Maglich et al. (*20*)], by approximately 85% in the DBD and 35% in the LBD (Figure 1a). The sequence was identical to the deduced amino acid sequence of flybase clone CG7404 (AF359420), except for the absence of two amino acid residues in positions 105 and 106. The numbering of amino acid residues was done according to our identified sequence in this paper.

Analysis of DNA Binding by Electrophoretic Mobility Shift Assay. The human and mouse ERRs are known to interact with two types of response elements. They bind DNA either to the single-repeat ERRE (TnAAGGTCA) or to the repeated ERE (AGGTCAnnnTGACCT) (*3*, *13*−*16*). To analyze the DNA binding properties of dERR, dERR and mERR proteins were synthesized by *in vitro* translation and analyzed by EMSA. Binding of the two receptors to labeled ERRE and ERE was tested, and unlabeled probes were used as competitors (Figure 1b,c). Mutated oligonucleotides were used as negative controls, and background controls were obtained by *in vitro* translation of pCDNA3 lacking an insert. dERR was shown to bind to the ERRE, and formation of the lower-molecular weight complex was competitively inhibited by unlabeled probe (Figure 1b). dERR was also shown to interact with the ERE, and unlabeled probe competitively inhibited the observed complexes (Figure 1c). These results agree with earlier studies on the DNA binding of the ERRs (*3*, *13*−*16*). The control, mERR, interacted with the ERRE and ERE (Figure 1b,c), also in agreement with earlier studies (*14*). Unlabeled probes were shown to successfully compete with the ERRE and the ERE probes for mERR binding (Figure 1b,c). Binding of dERR and mERR to the mutated probes (Figure 1b,c) could not be detected.

Transcriptional Activity of dERR. To analyze the transcriptional activity of the receptors, CaCo-2/TC7 and HEK293

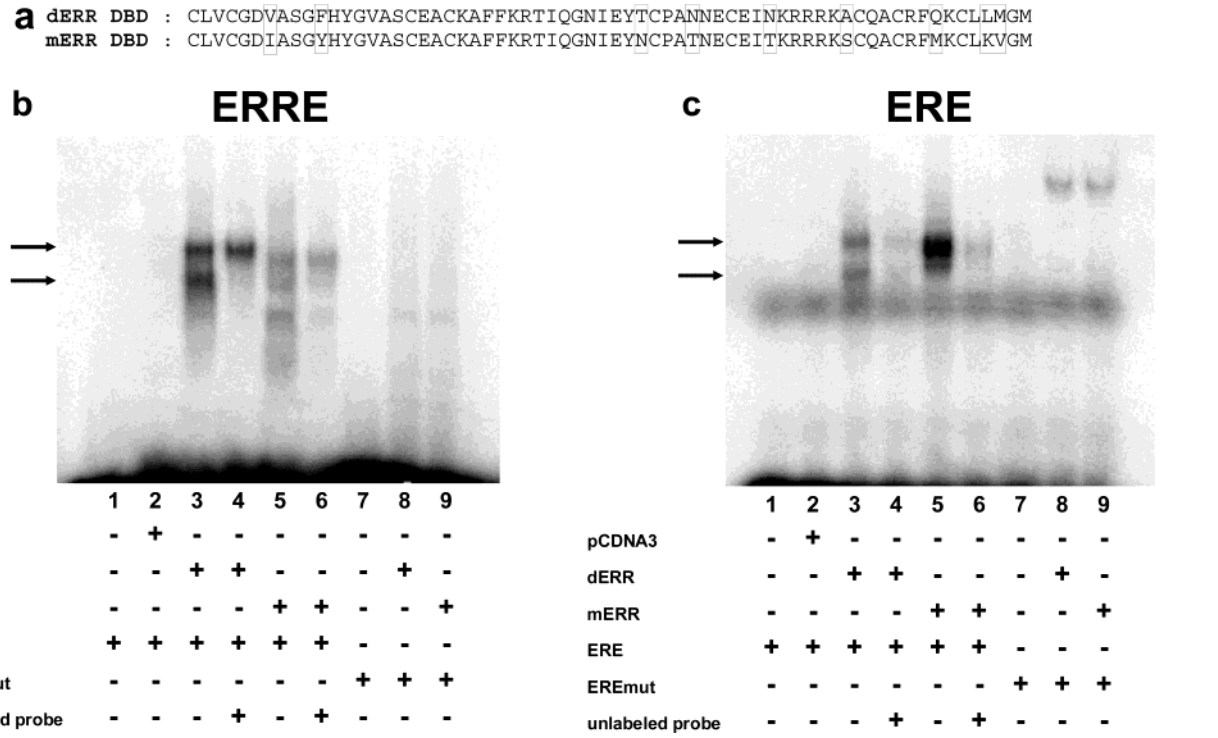

FIGURE 1: Alignment of dERR and mERR DBDs (a), with approximately 85% identical amino acids. Nonidentical amino acids are boxed. DNA binding of dERR and mERR to ERRE (b) and ERE (c) was analyzed by EMSA using proteins translated *in vitro*.

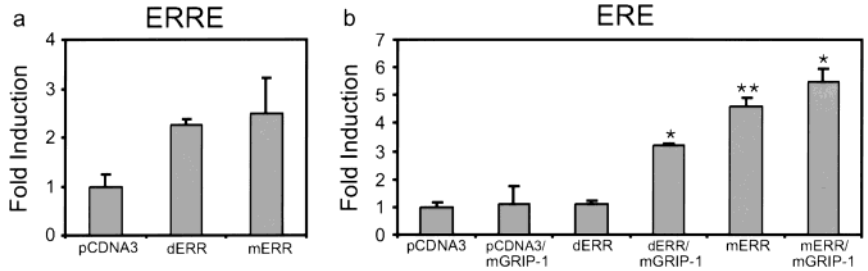

FIGURE 2: Transcriptional activity of dERR and mERR analyzed in CaCo-2/TC7 cells using full-length receptors. (a) The ERRE reporter plasmid was transfected in combination with pCDNA3 lacking an insert or expressing dERR or mERR as indicated. (b) The ERE reporter plasmid was transfected in combination with pCDNA3 lacking an insert or expressing dERR or mERR, with or without the mGRIP-1 expression plasmid, as indicated. The transfections were performed at least three times in duplicate. A typical experiment is shown. Data are shown as fold induction where luciferase activity was normalized for alkaline phosphatase activity and subsequently divided by reporter activity of pCDNA3 lacking an insert. Statistical analysis was carried out (Student's *t* test). Compared to pCDNA3, one asterisk means $P \leq 0.05$ and two asterisks mean $P \leq 0.01$.

cells were transfected with a full-length receptor construct and either an ERRE or an ERE reporter plasmid. Because of the high background generated with pCDNA3 lacking an insert and either of the reporter plamids in HEK293, likely originating from the presence of endogenous ERRs, this cell line was disregarded (data not shown). Using CaCo-2/TC7, the dERR and mERR receptors exhibited increased constitutive activity when transfected with the ERRE reporter plasmid (Figure 2a). Cotransfection of mGRIP-1 did not affect the activity (data not shown). In contrast, dERR exhibited no constitutive activity when cotransfected with the ERE reporter plasmid, while mERR exhibited significant constitutive activity with this reporter (Figure 2b). Cotransfection of mGRIP-1 increased the activity of dERR and to some extent also that of mERR (Figure 2b).

Transcriptional Activity of ERRs in the GAL4 System. Next, we examined whether dERR activity could be suppressed by known ERR inverse agonists. Here we used the GAL4 system, commonly used for NRs in the study of ligand-induced transcriptional activity (*26*). By using the GAL4 system, ligand-dependent effects originating from endogenous ERs/ERRs were avoided. The cell lines evaluated for the cell-based reporter assays were HEK293 and CaCo-2/TC7. The latter cell line was chosen because of a better signal-to-noise ratio when tested for the LBD constructs. CaCo-2/TC7 cells were transiently transfected with a GAL4−dERR LBD fusion construct and a 4xGAL4-RE luciferase reporter, and subsequently treated with the known ERR inverse agonists 4-hydroxytamoxifen (OHT), diethylstilbestrol (DES), and tamoxifen (TAM). dERR exhibited constitutive activity [like ERRα (*7*, *10*)] which was slightly suppressed by 10 μM OHT (Figures 3a and 8a) and 10 μM DES (Figures 3a and 8b). In comparison, the activity of mERRβ was significantly suppressed by 10 μM OHT and DES (Figure 3b) as expected (*9*, *10*). At a lower concentration (1 μM), OHT and DES (Figure 3b) still suppressed the activity of mERR efficiently. TAM (10 μM) suppressed

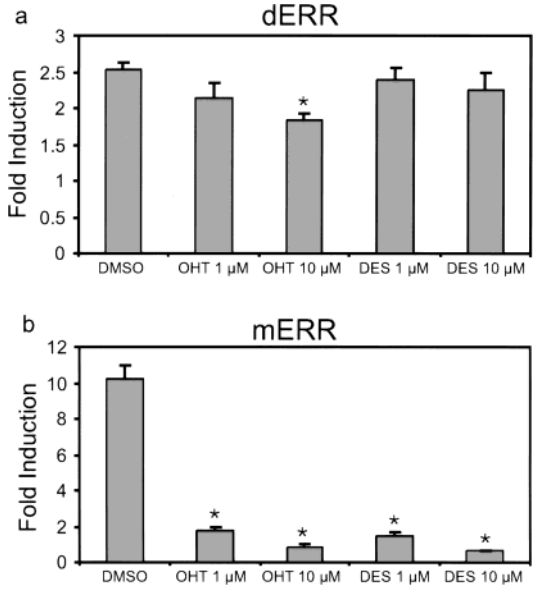

FIGURE 3: Ligand modulation of dERR activity. Transfections of GAL4−LBD fusion plasmids in combination with the 4xGAL4-RE luciferase reporter plasmid were performed. Cells transfected with dERR (a) or mERR (b) were treated with OHT or DES at a final concentration of 10 or 1 μM as indicated. The transfections were performed at least three times in duplicate. A typical experiment is shown. Data are shown as fold induction where luciferase activity was normalized for alkaline phosphatase activity and subsequently divided by the reporter activity of pCMXGal4. Statistical analysis was carried out (Student's *t*-test). Compared to DMSO, one asterisk means $P \leq 0.05$.

mERR efficiently but had no effect on dERR (data not shown).

Homology Modeling and Docking. The inefficient suppression of dERR activity by known ERR inverse agonists led us to a closer examination of the differences in the ligand binding pockets of dERR and mammalian ERRs and ERs. On the basis of the hypothesis that amino acid differences in the ligand binding pockets of the ERRs/ERs and dERR contribute to the inefficient suppression of dERR by 4-hydroxytamoxifen (OHT), a homology model of dERR LBD was created using the ICM software (*28*). To produce a model of dERR in a putative inactive state, the structure of human ERα bound to OHT [Protein Data Bank (PDB) entry 3ert (*22*)] was used as a template. hERα was the closest homologue in the database at this time. All amino acid residues in the model within 5.0 Å of OHT were identified (Figure 4). Since OHT binds to hERα and antagonizes its coactivator interaction (*22*), the similarities and differences between the ligand binding pockets of hERα and dERR are interesting. Our homology model of dERR LBD (Figure 5) suggested a pocket similar to that of ERα, and three potentially interesting differences (Figure 6) were observed, namely, amino acid residues Y295, T333, and Y365. Figure 6 clearly shows that Y295 almost completely fills the space in the ligand binding pocket, which therefore cannot be occupied by OHT. The model further suggests that T333 and Y365 also contribute to the inefficient suppression of dERR activity by OHT, since T333 and Y365 are polar residues in a region which is mostly hydrophobic in hERα, and Y365 is more bulky than the equivalent methionine residue in hERα. We proceeded to construct mutants of these three residues based on the hypothesis that they were involved in the OHT response of hERα. A single mutant Y295A, a double mutant T333I/Y365L, and a triple mutant Y295A/T333I/Y365L were created. Isoleucine and leucine were chosen since these are the corresponding residues in the three human ERRs, with the exception that T333 corresponds to a valine in hERRα.

To further test this hypothesis *in silico*, OHT and DES were docked to the wild-type dERR LBD and to two of the mutant dERR LBD models (Y295A and Y295A/T333I/Y365L). We hypothesized that if the docking program [ICM (*29*)] would be able to automatically dock the compounds into the binding pocket of the mutants but not to the wild-type protein, this would indicate that the mutations enable OHT and DES to bind to the dERR mutants *in vitro*. Figure 7a shows that OHT cannot fit into the pocket of the wild-type protein, while it probably can fit sterically into the single mutant. However, the lower lipophilicity of the single mutant, compared to that of hERα, resulted in a different docking mode. In contrast, OHT docked to the triple mutant in a manner similar to the binding mode observed in the hERα−OHT cocrystal structure (*22*), with the hydrophobic, bulky part of the ligand inside the pocket and the aminoethoxy side chain protruding outward, toward helix 12. DES was also predicted not to fit into the binding pocket of the wild-type protein. DES was predicted to bind in the same manner to both the single mutant and the triple mutant, but the increased lipophilicity of the triple mutant probably increases the affinity of the triple mutant for DES compared to that of the single mutant (Figure 7b).

Transcriptional Activity of GAL4−dERR LBD Mutants. To examine whether the mutations increased the susceptibility to OHT as suggested by the modeling, CaCo-2/TC7 cells were transiently transfected with pCMX vectors encoding GAL4 fusions of the triple (Y295A/T333I/Y365L), double (T333I/Y365L), and single (Y295A) dERR mutants and the 4xGAL4-RE luciferase reporter. The constitutive activity of all three mutants was lower compared to the wild-type dERR level (Figure 8). The single mutant Y295A was significantly suppressed by OHT and DES at a concentration of 10 μM, but not at 1 μM (Figure 8a,b). The triple mutant was significantly suppressed by both of the substances at 10 μM, whereas 1 μM OHT more efficiently suppressed the activity of the triple mutant than 1 μM DES (Figure 8a,b). The double mutant was not significantly suppressed by any of the substances (Figure 8a,b). Titration of OHT dose-dependently suppressed the activity of the triple mutant in a concentration range from 0.6 to 10 μM (data not shown).

Finally, the interaction between mutant dERRs and the coactivator mGRIP-1 was analyzed. When cotransfected with mGRIP-1, mutants as well as wild-type dERR exhibited increased constitutive activity (data not shown), indicating that the mutants have retained functional coactivator interaction. To verify the ability of ligand-dependent suppression of this increased activity, cells cotransfected with the triple (Y295A/T333I/Y365L) mutant and the coactivator mGRIP-1 were treated with 10 μM OHT. As seen in Figure 9, the activity of the triple mutant (Y295A/T333I/Y365L) cotransfected with mGRIP-1 was efficiently repressed by OHT, indicating that the coactivator is released upon interaction between OHT and the triple mutant receptor.

```
                                                        *  **  ** *
hERa 306 : --LALSLTADQMVSALLDAEPPILYSEYDPTRPFSEASMMGLLTNLADRELVHMINWAKR : 363
dERR 252 : DEASSSSGSIKLESSVVTPNGTCIFQNNNNNDP---NEILSVLSDIYDKELVSVIGWAKQ : 308
hERa SS  :   _HHH__HHHHHHHHHH_____________________HHHHHHHHHHHHHHHHHHHHH
dERR SS  : _____________HHH_________________H   HHHHHHHHHHHHHHHHHHHHHHH

                                *   **  **  *         *                **
hERa 364 : VPGFVDLTLHDQVHLLECAWLEILMIGLVWRSMEHPGKLLFAPNLLLDRNQGK-CVEGMV : 422
dERR 309 : IPGFIDLPLNDQMKLLQVSWAEILTLQLTFRSLPFNGKLCFATDVWMDEHLAKEC--GYT : 366
hERa SS  :   ___HHH__HHHHHHHHHHHHHHHHHHHHHH_____EEEEE__EEEEHHHHH H_____
dERR SS  :   _____EE_HHHHHHHHHHHHHHHHHHHHHH_____EEEE____EE_HHH____  ___

hERa 423 : EIFDMLLATSSRFRMMNLQGEEFVCLKSIILLNSGVYTFLSSTLKSLEEKDHIHRVLDKI : 482
dERR 367 : EFYYHIVQIAQRMERISPRREEYYLLKALLLANCDI---------LLDDQSSLRAFRDTI : 417
hERa SS  : _HHHHHHHHHHHHHH___HHHHHHHHHHHHHH___________HHHHHHHHHHHHHHHHH
dERR SS  : HHHHHHHHHHHHHHH____HHHHHHHHHHHHH____        ____HHHHHHHHHH

                                                    ** **    *     *
hERa 483 : TDTLIHLMAKAGLTLQQQHQRLAQLLLILSHIRHMSNKGMEHLYSMKCKNVVPLYDLLLE : 542
dERR 418 : LNSLNDVVY--LLRHSSAVSHQQQLLLLLPSLRQADDILRRFWRGIARDEVITMKKLFLE : 475
hERa SS  : HHHHHHHHHH____HHHHHHHHHHHHHHHHHHHHHHHHHHHHHHHH_______HHHHHHH
dERR SS  : HHHHHHHHH  H_________HHHHHHHHHHHHHHHHHHHHHHHHHHHH_________HHHHH

hERa 543 : MLDAHRLHAP : 552
dERR 476 : MLEPLAR--- : 482
hERa SS  : HH________
dERR SS  : HH_____
```

FIGURE 4: Sequence alignment and secondary structure (marked ss in the alignment) prediction used for constructing the dERR homology model based on hERα. The alignment shows 27.7% amino acid identity. Identical residues are highlighted in black, and conserved residues are highlighted in gray. The alignment was rendered using GeneDoc [http://www.psc.edu/biomed/genedoc/; Nicholas, K. B., and Nicholas, H. B., Jr. (1997) *GeneDoc: Analysis and Visualization of Genetic Variation*]. The secondary structure of hERα was taken from PDB entry 3ert (*22*), and the secondary structure of dERR was predicted using PSI-PRED (*32*). Residues within 5.0 Å of OHT and having more than 5% surface accessibility are marked with asterisks. The residues marked with asterisks that were selected for engineering are highlighted in gray. H denotes helices and E β-sheets. Residues are considered homologous according to the PAM250 substitution matrix, giving the following amino acid groupings: DENQH, SAT, KR, FY, and LIVM.

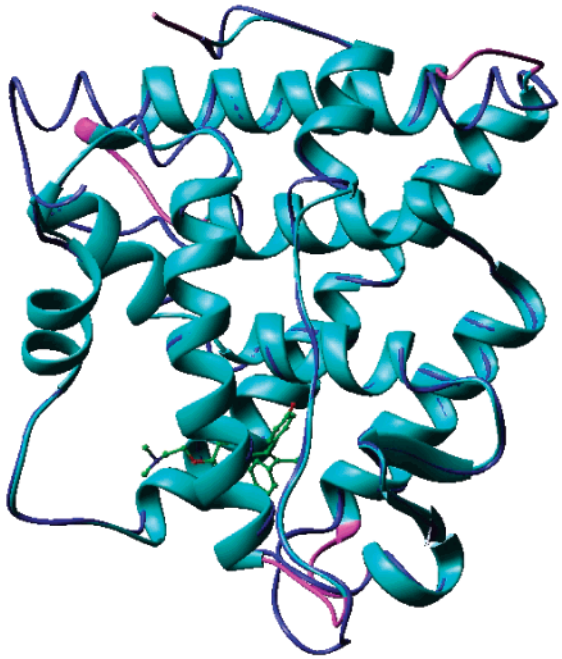

FIGURE 5: Generated homology model of dERR LBD, with the template structure (hERα) shown in blue. OHT from 3ert (*22*) is shown in green. The parts of the model treated as gaps are shown in magenta.

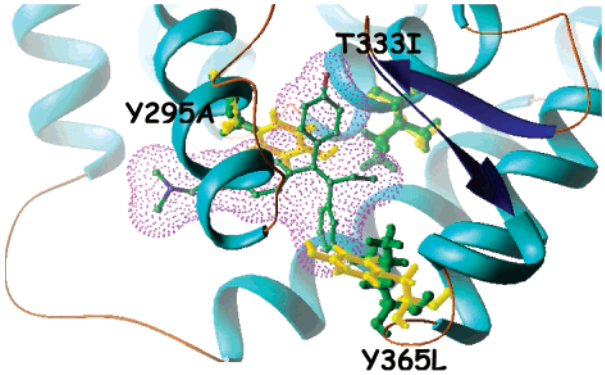

FIGURE 6: Close-up view of OHT in the ligand binding pocket of the dERR model, placed as in the hERα OHT cocrystal structure. Three residues were mutated to increase the affinity of OHT for dERR. Wild-type dERR amino acid residues are shown in yellow and mutant residues in green.

DISCUSSION

We have cloned and verified the sequence of the novel member of the NR3 family, dERR [previously reported (*20*)], and performed functional studies of wild-type and mutant receptors by *in vitro* assays. In this report, we demonstrate the rational design of ligand-induced suppression of this receptor, based on homology modeling and *in silico* docking.

Functional Analysis of dERR. The results from the EMSA indicate that dERR is able to bind both ERE and ERRE *in vitro*. The nature of the observed higher-molecular weight complex, which could not be inhibited by unlabeled probe, is unknown (Figure 1b). It should be noted that others have observed additional stimulating factors present in serum bound to ERR−DNA complexes (*30*). It is possible that the observed higher-molecular weight complex in our study originates from an additional component present in the reticulocyte lysate; however, further elucidating the nature of this complex and how it affects DNA binding would

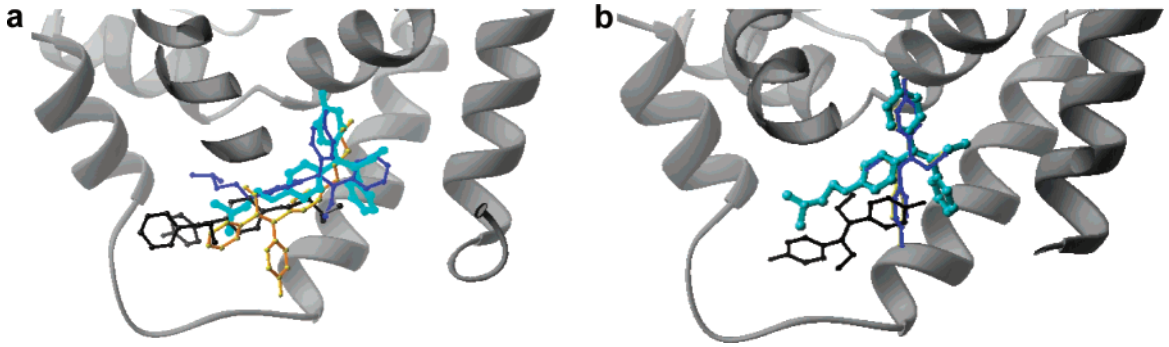

FIGURE 7: Comparison of ligand docking in different dERR models. (a) OHT was automatically docked to the model of wild-type dERR (black), the Y295A single mutant (gold), and the Y295A/T333I/Y365L triple mutant (blue). OHT derived from the cocrystal structure with hERα is shown in cyan. (b) Analogous docking results for DES, where the docking to the model of Y295A and Y295A/T333I/Y365L is more or less similar and therefore overlaps. The figures were generated using Ribbons (*38*).

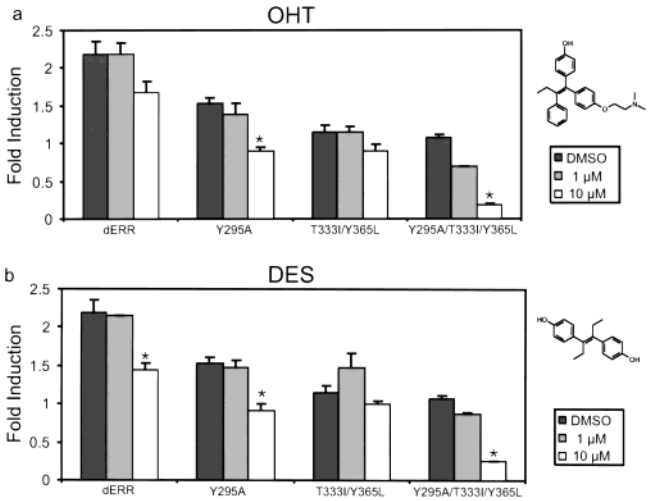

FIGURE 8: Ligand modulation of mutant dERR activity using transfections, performed as described in the legend of Figure 3. Transfected cells were treated with OHT (a) or DES (b) and DMSO at the indicated concentrations. Respective structures are shown to the right. Statistical analysis was carried out (Student's *t* test). Compared to DMSO, one asterisk means $P \leq 0.05$.

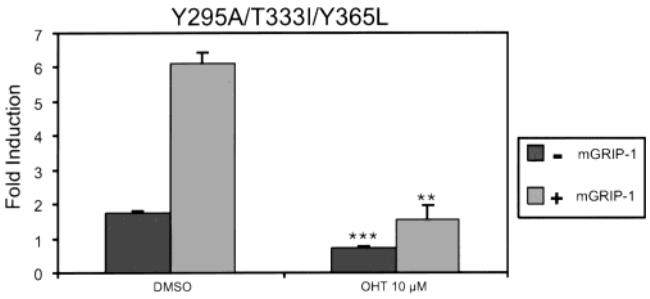

FIGURE 9: Effect of mGRIP-1 on the activity of the triple mutant and suppression by OHT. Cells were transfected as described in the legend of Figure 3 with the dERR triple mutant and mGRIP-1 as indicated, and treated with 10 μM OHT or DMSO. Statistical analysis was carried out (Student's *t* test). Compared to DMSO, one asterisk means $P \leq 0.05$, two asterisks mean $P \leq 0.01$, and three asterisks mean $P \leq 0.001$.

require more detailed studies. Results from transfection experiments revealed that dERR is able to activate transcription through the ERRE and ERE in a human cell line. This indicates a conserved mechanism of transcriptional activation for NRs within the NR3 subfamily. Also, the mechanism of coactivator recruitment seems to be conserved for the ERRs, as indicated by our transfection experiments.

Homology Modeling of the dERR LBD. The fact that dERR responded poorly to the known ERR inverse agonists led us to compare the ligand binding pockets of the dERR, ERRs, and ERs, to identify crucial amino acid residues that could be involved in the different observed responses. The crucial issue of homology modeling is the choice of template and the construction of the alignment. hERα (*22*) is the structure most homologous to dERR present in a relevant holo form in the PDB. A structure of human hERR3 was recently reported [PDB entry 1kv6 (*31*)]. hERR3 is more homologous to dERR than hERα; however, the crystal structure of hERR3 is in its apo form as opposed to the hERα structure (*22*), and therefore, the crystal structure of hERα was used as a template. The alignment of dERR and hERα is not trivial, in particular, the placing of helix 1 and the position of the gap between helices 8 and 9. Because of the relatively low level of homology (<30% identical), emphasis was put on matching predicted (*32*) secondary structure elements and using multiple alignments of dERR orthologues and homologues. The resulting alignment is quite consistent with the alignment between hERR3 and hERα presented by Greschik et al. (*31*), with slightly different gaps, suggesting that the ligand binding pocket of our model is more or less correctly predicted. The resulting model is well relaxed in the force field used during modeling, with no significant high-energy contacts. To evaluate the protein-likeness of the model, PROCHECK (*33*) was used. In the Ramachandran plot, 191 of 214 non-Gly and non-Pro residues are in the most favored region, only one residue is in the disallowed region, one is in the generously allowed region, and the number of bad contacts is five, which is comparable to the statistics of a typical high-resolution crystal structure.

Mutational Analysis. Transfection experiments with the wild-type dERR construct revealed that the activity of the receptor is inefficiently suppressed by the known ERR inverse agonists OHT, TAM, and DES. These results are in agreement with our model of the wild-type dERR LBD where OHT cannot dock into the ligand binding pocket of dERR due to sterical hindrance. This is probably due to the side chain of Y295 filling out the space where OHT would presumably bind (Figure 7). As expected, the mutation of Y295 into an alanine results in stronger suppression of the receptor by OHT as well as DES and TAM. In addition, this mutation was also shown to lower the constitutive activity as compared to that of wild-type dERR (Figure 8). This agrees with results from previous studies of ERRα

where a F329A mutant loses its transcriptional activity (*34*). An explanation for this phenomenon could be that the side chain of Y295 stabilizes the protein. The active conformation of dERR is probably one where H12 is folded back over the putative ligand binding pocket, forming close contacts with H4, in accordance with the general mechanism of NR LBD activation (*35*). These results suggest that Y295 normally occupies a large proportion of the putative ligand binding pocket, and changing it to an alanine decreases the stability of the active conformation and hence decreases the basal activity of the receptor and simultaneously opens the LBD for ligand binding. Our results are supported by earlier studies of the corresponding amino acid residues in hERα (*9*, *34*), hERR*β*, hERR*γ* (*9*, *10*), and hERRα (*9*). Taken together, these results identify this amino acid residue as being important in ligand binding as well as transactivation. The results from the reporter gene assays revealed that the T333I and Y365L mutations are not by themselves sufficient for suppression of OHT, but result in a decrease in the constitutive activity of the receptor, likely by destabilization of the protein. This indicates that the active conformation of wild-type dERR might be stabilized by hydrogen bonding of T333 and Y365, thereby making the structure more compact (*35*).

The triple mutant Y295A/T333I/Y365L was shown to be more efficiently suppressed by OHT than the single mutant, as predicted in our models. As discussed earlier, the substitution of the tyrosine with an alanine removes sterical hindrance and creates a void in which OHT can bind. The fact that the triple mutant is more efficiently suppressed than the single mutant suggests that the two hydrophobic substitutions make the ligand binding pocket more favorable for binding of OHT. Finally, cotransfection of the triple mutant and mGRIP-1 resulted in a 3-fold increase in the constitutive activity. This shows that the ability to interact with a coactivator is indeed still maintained by the triple mutant, in turn suggesting that the introduced mutations do not seriously perturb the protein from its native structure.

In conclusion, our studies provide the first functional characterization of both the wild-type and engineered variants of the recently identified dERR. dERR has been suggested as an ancestor of the NR3 subfamily of steroid receptors (*20*, *36*). This raises the question of the existence of a natural ligand for dERR, or if ligand responsiveness in the NR3 family of steroid hormone receptors has been acquired later in evolution. So far, no natural ligands for the ERRs have been identified, but a few synthetic ligands that suppress the constitutive activity of the ERRs have been reported (*7*, *9*−*11*). The size of the dERR ligand binding pocket in our model indicates that the pocket is too small for a ligand to fit. However, structural flexibility of the ligand binding pocket of nuclear receptors has previously been suggested as a way for the pocket to accommodate ligands of different sizes (*37*). Further studies are needed to determine if ligand binding to wild-type dERR is possible. An alternative to traditional screening methods for identifying potential ligands of dERR could be the docking of a large set of substances to a LBD model *in silico*. However, this would probably require a more detailed model or structure of the dERR LBD (*29*).

Our results demonstrate the potential of rational design and engineering of NR LBDs in the study of the function of receptors lacking defined ligands by introducing a limited number of site specific mutations that confer ligand responsiveness. As an increasing number of crystal structures of NRs in complex with ligands become available, it will be possible to more accurately predict such site specific mutations for functional analysis of other orphan nuclear receptors. This is useful in the elucidation of ligand-modulated activities and functions of the receptor, as well as a guidance tool for structure-based design of new synthetic compounds targeting nuclear receptors.

ACKNOWLEDGMENT

We thank Annelie Sjögren for the cloning of dERR and Sven-Åke Franzén, Andrea Varadi, and Marianne Israelsson for DNA sequence analysis. Patrik Blomquist, Thomas Perlmann, and Jonas Uppenberg are acknowledged for critical reading of the manuscript. The mGRIP-1 plasmid was a generous gift from Dr. Eckardt Treuter (CBT, Karolinska Institute). The TC7 subclone of CaCo-2 cells was kindly provided by Dr. Monique Rousset (Institut National de la Santé et de la Recherche Médicale U178, Villejuif, France).

REFERENCES

1. Giguère, V., Yang, N., Segui, P., and Evans, R. M. (1988) *Nature 331*, 91−94.
2. Laudet, V., Auwerx, J., Gustafsson, J.-Å., and Wahli, W. (1999) *Cell 97*, 161−163.
3. Yang, N., Shigeta, H., Shi, H., and Teng, C. T. (1996) *J. Biol. Chem. 271*, 5795−5804.
4. Eudy, J. D., Yao, S., Weston, M. D., Ma-Edmonds, M., Talmadge, C. B., Cheng, J. J., Kimberling, W. J., and Sumegi, J. (1998) *Genomics 50*, 382−384.
5. Heard, D. J., Norby, P. L., Holloway, J., and Vissing, H. (2000) *Mol. Endocrinol. 14*, 382−392.
6. Hong, H., Yang, L., and Stallcup, R. (1999) *J. Biol. Chem. 274*, 22618−22626.
7. Tremblay, G. B., Kunath, T., Bergeron, D., Lapointe, L., Champigny, C., Bader, J. A., Rossant, J., and Giguère, V. (2001) *Genes Dev. 15*, 833−838.
8. Xie, W., Hong, H., Yang, N. N., Lin, R. J., Simon, C. M., Stallcup, M. R., and Evans, R. (1999) *Mol. Endocrinol. 13*, 2151−2162.
9. Coward, P., Lee, D., Hull, M. V., and Lehmann, J. M. (2001) *Proc. Natl. Acad. Sci. U.S.A. 98*, 8880−8884.
10. Tremblay, G. B., Bergeron, D., and Giguere, V. (2001) *Endocrinology 142*, 4572−4575.
11. Yang, C., and Chen, S. (1999) *Cancer Res. 59*, 4519−4524.
12. Soto, A. M., Sonnenschein, C., Chung, K. L., Fernandez, M. F., Olea, N., and Serrano, F. O. (1995) *Environ. Health Perspect. 103*, 113−122.
13. Johnston, S. D., Liu, X., Zuo, F., Eisenbraun, T. L., Wiley, S. R., Kraus, R. J., and Mertz, J. E. (1997) *Mol. Endocrinol. 11*, 342−352.
14. Lu, D., Kiriyama, Y., Lee, K. Y., and Giguere, V. (2001) *Cancer Res. 61*, 6755−6761.
15. Pettersson, K., Svensson, K., Mattsson, R., Carlsson, B., Ohlsson, R., and Berkenstam, A. (1996) *Mech. Dev. 54*, 211−223.
16. Sladek, R., Bader, J.-A., and Giguere, V. (1997) *Mol. Cell. Biol. 17*, 5400−5409.
17. Laudet, V. (1997) *Mol. Endocrinol. 19*, 207−226.
18. Rubin, G. M., Yandell, M. D., Wortman, J. R., Gabor Miklos, G. L., Nelson, C. R., Hariharan, I. K., Fortini, M. E., Li, P. W., Apweiler, R., Fleischmann, W., et al. (2000) *Science 287*, 2204−2215.
19. Sluder, A. E., Mathews, S. W., Hough, D., Yin, V. P., and Maina, C. V. (1999) *Genome Res. 9*, 103−120.
20. Maglich, J. M., Sluder, A., Guan, X., Shi, Y., McKee, D. D., Carrick, K., Kamdar, K., Willson, T. M., and Moore, J. T. (2001) *GenomeBiology 2*, 0029.1−0029.7.

21. Thummel, C. S. (1995) *Cell 83*, 871−877.
22. Shiau, A. K., Barstad, D., Loria, P. M., Cheng, L., Kushner, P. J., Agard, D. A., and Greene, G. L. (1998) *Cell 95*, 927−937.
23. Laudet, V., Hänni, C., Coll, J., Catzeflis, F., and Stéhelin, D. (1992) *EMBO J. 11*, 1003−1013.
24. Eddy, S. R. (1995) *Proc. Int. Conf. Intell. Syst. Mol. Biol. 3*, 114−120.
25. Grandien, K. (1996) *Mol. Cell. Endocrinol. 116*, 207−212.
26. Perlmann, T., and Jansson, L. (1995) *Genes Dev. 9*, 769−782.
27. Bertilsson, G., Heidrich, J., Svensson, K., Åsman, M., Jendeberg, L., Sydow-Bäckman, M., Ohlsson, R., Postlind, H., Blomquist, P., and Berkenstam, A. (1998) *Proc. Natl. Acad. Sci. U.S.A. 95*, 12208−12213.
28. Abagyan, R. A., and Totrov, M. M. (1994) *J. Mol. Biol. 235*, 983−1002.
29. Schapira, M., Raaka, B. M., Samuels, H. H., and Abagyan, R. (2000) *Proc. Natl. Acad. Sci. U.S.A. 97*, 1008−1013.
30. Hentschke, M., Süsens, U., and Borgmeyer, U. (2002) *Eur. J. Biochem. 269*, 4086−4097.
31. Greschik, H., Wurtz, J. M., Sanglier, S., Bourguet, W., van Dorsselaer, A., Moras, D., and Renaud, J. P. (2002) *Mol. Cell 9*, 303−313.
32. Jones, D. T. (1999) *J. Mol. Biol. 292*, 195−202.
33. Laskowski, R. A., MacArthur, M. W., Moss, D. S., and Thornton, J. M. (1993) *J. Appl. Crystallogr. 26*, 283−291.
34. Chen, S., Zhou, D., Yang, C., and Sherman, M. (2001) *J. Biol. Chem. 276*, 28465−28470.
35. Wurtz, J. M., Bourguet, W., Renaud, J. P., Vivat, V., Chambon, P., Moras, D., and Gronemeyer, H. (1996) *Nat. Struct. Biol. 3*, 87−94.
36. Giguere, V. (2002) *Trends Endocrinol. Metab. 13*, 220−225.
37. Watkins, R. E., Wisely, G. B., Moore, L. B., Collins, J. L., Lambert, M. H., Williams, S. P., Willson, T. M., Kliewer, S. A., and Redinbo, M. R. (2001) *Science 292*, 2329−2333.
38. Carson, M. (1991) *J. Appl. Crystallogr. 24*, 958−961.

BI027279B